

I) Operational NWP system & satellite usage

- Global:**
 - ICON, non-hydrostatic, 13 km, 90 σ -z-levels up to 70 km (~2.6 Pa)
 - 3DVar for conventional and satellite data, 3h cycling
- Regional:**
 - COSMO-EU: 7 km, 40 Levels (up to ~22 km, non-hydrostatic) to be replaced by ICON-EU-Nest in Q1/2016 (see panel II)
 - COSMO-DE: 2.8 km, 50 Levels (non-hydrostatic)
 - COSMO-DE-EPS ensemble at 2.8 km, 40 members
 - Nudging assimilation scheme for conventional and radar data
- Satellite data/global ICON:**
 - AMSU-A (chan 9-14 everywhere, 5-8 only over sea), ATMS (similar, 3*3 superobbing)
 - HIRS (chan 4-7, 14, 15, over sea), IASI (45 chan, McNally&Watts cloud detection, over sea)
 - AMSU-B/MHS pre-operational
 - GPS-RO bending angles
 - AMVs (GEO, LEO), Scatterometer winds
 - Monitoring of AMSR-2, Meteosat CSR, JASON-2 winds
- Technical aspects:**
 - RTTOV-10
 - Flexible satellite data ingestion & pre-processing package
 - Monitoring: Automatic problem detection & alert system
 - Online bias correction
- Current developments:**
 - Operational introduction of VarBC
 - Extended IASI usage; introduction of humidity sensitive radiances
 - QC/cloud screening: New observation cross-validation method, see **Poster 8p.05 and Presentation 11.06 (O. Stiller)**
 - Analysis of surface emissivity and skin temperature

II) Radiance assimilation in ICON

The **ICON model (ICOsahedral Nonhydrostatic modelling framework)**, developed in cooperation between DWD and the MPI for climate research (Hamburg) is providing **global operational forecasts at DWD since 20 Jan 2015 on a 13 km icosahedral grid** (Fig. 1) with **90 vertical σ -z-levels**. The global runs simultaneously provide forecasts at **6.5 km over a European domain (ICON-EU)** through a two-way nesting. ICON also provides a greatly improved basis for radiance assimilation, especially due to a significantly raised **model top (at 70 km, ~2.6 Pa)** and a highly improved physics parameterizations package.

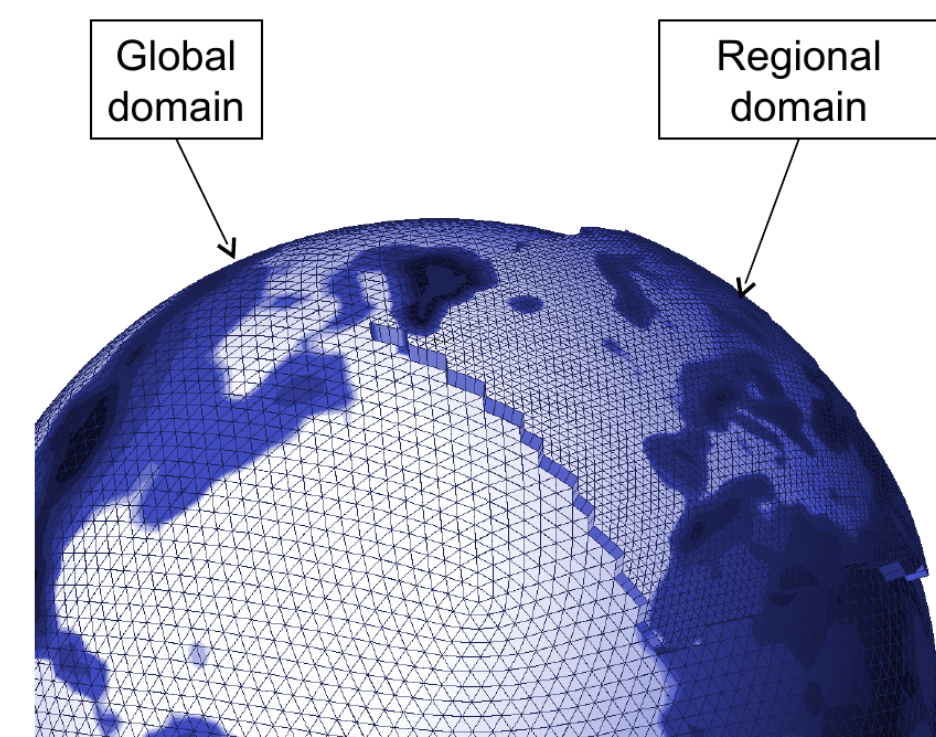


Fig 1: Schematic diagram of ICON grid with regional two-way nest.

The introduction of this completely new model (both in dynamics and physics) required an intensive tuning period concerning the interaction between used observations, the data assimilation system setup, and especially the model physics. A selection of results and interactions observed concerning the assimilation of satellite radiances are discussed in **Poster 11p.08**.

The **forecast impact of radiances** in the 3DVar/ICON setup on its introduction in January 2015 is illustrated in Fig. 2. Current work focuses on enhancing this impact through improved bias correction (VarBC) and the assimilation of additional instruments on top of the currently still limited set of radiances. Further improvements are expected through the introduction of an EnVAR assimilation system in the near future (see III) due to a much more realistic description of the background error covariances.

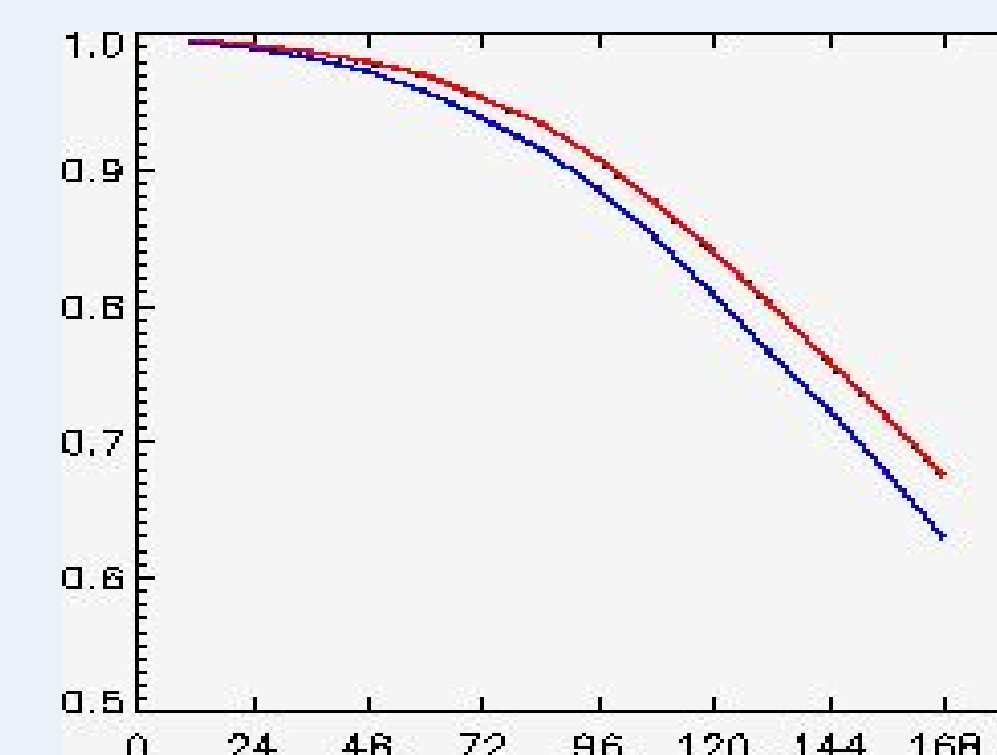


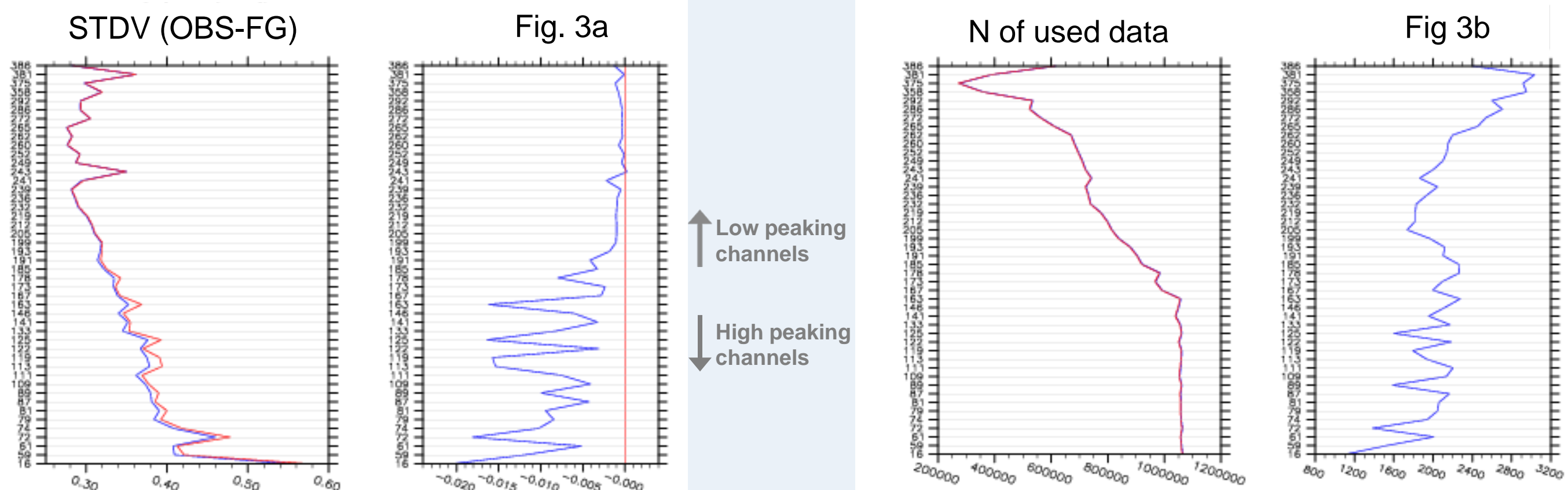
Fig 2: Forecast anomaly correlation for SH, 500 hPa geopotential for the full setup (at ICON introduction Jan 2015) versus forecast time (in h) and a withdrawal experiment without radiances (3 month period).

Other updates during the last two years include:

- Introduction of ATMS (June 2014)
- Introduction of IASI from METOP-A/B (July 2014)
- Use of high-peaking AMSU & ATMS channels (9-14) above thick cloud and over land (Sep 2015)
- Increased number of instruments in monitoring (AMSR-2, Meteosat CSR, JASON-2)

Fig 3a (left): Standard deviation (left panel) of OBS-FG for used IASI channels in two experiments and relative difference of stdv between experiments (right panel). Red: setup with AMSU&ATMS only over sea and thin cloud (low LWP) conditions; Blue: high-peaking AMSU&ATMS channels 9-14 assimilated also over land and in areas with thick cloud or rain.

Fig 3b (right): Number of IASI observations used per channel (left panel) and difference between experiments (right panel).



The assimilation of high-peaking AMSU & ATMS channels everywhere leads to a consistent improvement in short range forecasts, visible in the fit of the FG to other observations like e.g. IASI, radiosondes. Improvements in forecast scores were visible particularly over northern high latitudes and in Europe.

IV) Satellite data for convective-scale assimilation using ensemble data assimilation (LETKF)

For regional high resolution analyses, the **KENDA system** (km-scale ensemble-based data assimilation) based on the **LETKF** (Hunt et al.) is being developed and will replace the current nudging scheme. Current development direction focuses on tuning, adaptive localization and the exploitation of additional, particularly remote sensing, observations:

- Volume radar scans (implementation of 3D forward operator)
- GPS (slant) delays
- Cloud information and cloudy radiances from SEVIRI (METEOSAT)
- Assimilation of SEVIRI visible channel radiances, see **Poster 2p.08 (L. Scheck)**

III) Introduction of EnVar assimilation

The **current development** focuses on the implementation of the new **EnVAR ensemble data assimilation** system, which consists of a coupling between a global (lower resolution) LETKF ensemble data assimilation, providing flow dependent background errors, and a full resolution deterministic 3DVar. The following setup is running continuously in the pre-operational testing and tuning and initial evaluation show significantly improved forecast scores.

- **Global LETKF:** at 40 km, 40 members, ICON model
- **Global EnVAR:** at 13 km, deterministic 3DVar using flow-dependent B matrix from LETKF ensemble blended with a climatological B
- **Global EPS:** 40 members from global LETKF ensemble, forecasts up to 120 h (00, 12 UTC); additionally for 24h every 3h to provide boundaries to regional LETKF
- **Regional LETKF:** at 2.8 km, 40 members, COSMO-DE model
- **Regional EPS:** COSMO-DE at 2.8 km, 20 Members, (not yet initialized from LETKF analyses)

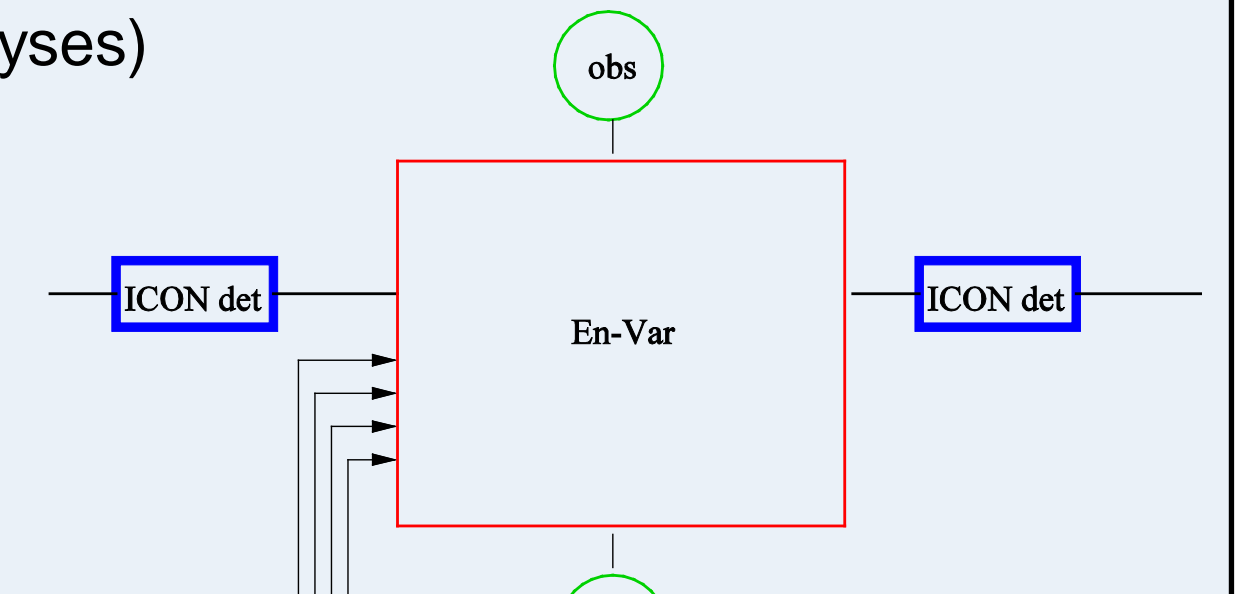


Fig 4 (right): Schematic diagram of the interaction between the global ensemble prediction (ICON ens) and analysis (LETKF) and the deterministic forecast (ICON det) with the EnVar analysis. The EnVar uses the flow-dependent background errors from the ensemble. The observation processing and quality control (QC) are performed only once by the EnVar and used in the ensemble LETKF analysis.

Fig 5 (below): Illustration of the flow-dependent background errors provided through the LETKF with the spread of T (left) and the cross-correlations between T and Qv (right) at around 500 hPa for 30 May 2015 as example. Both the situation dependent size of the background errors (low in e.g. well observed areas and much higher in dynamically active areas) and the multivariate nature of B with cross-correlations between the different physical variables (here T and Qv) are clearly visible.

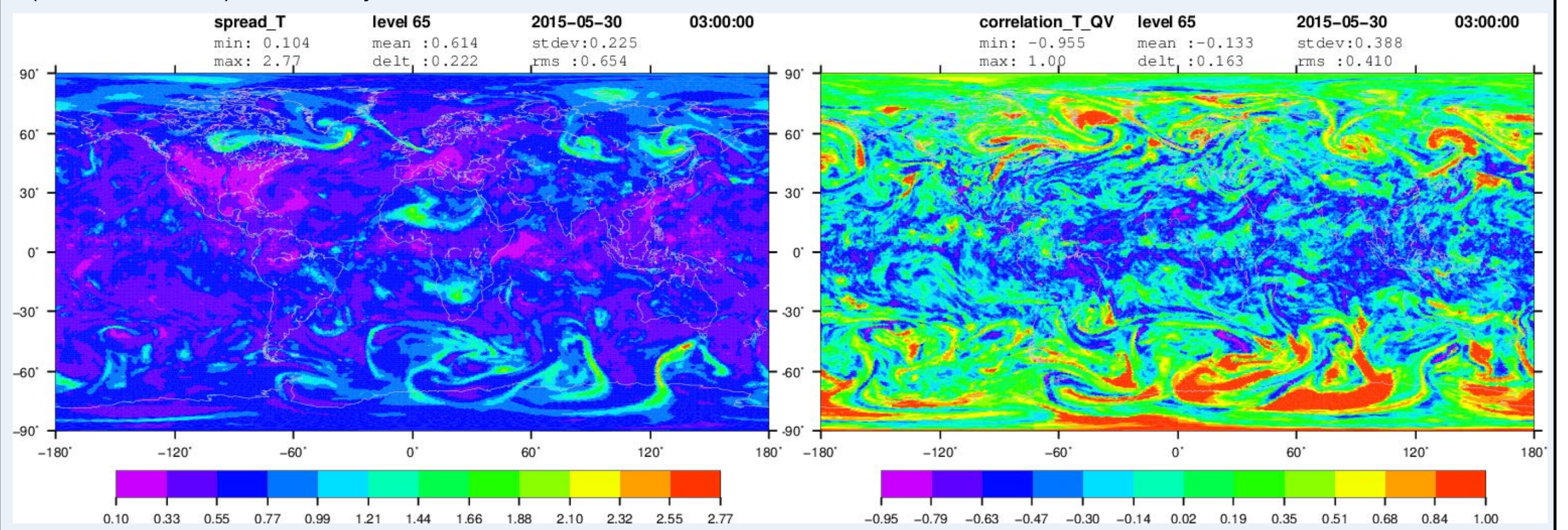
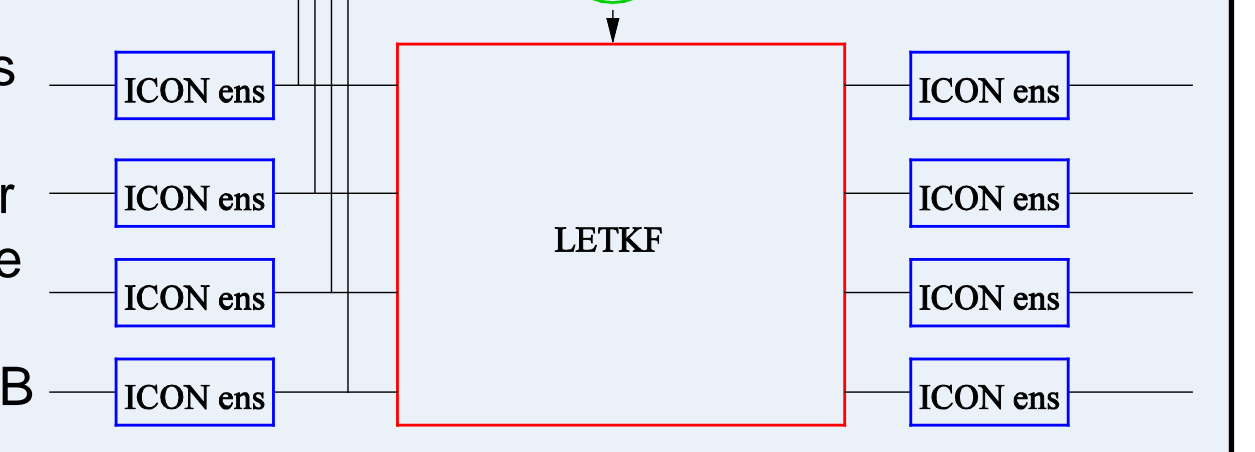
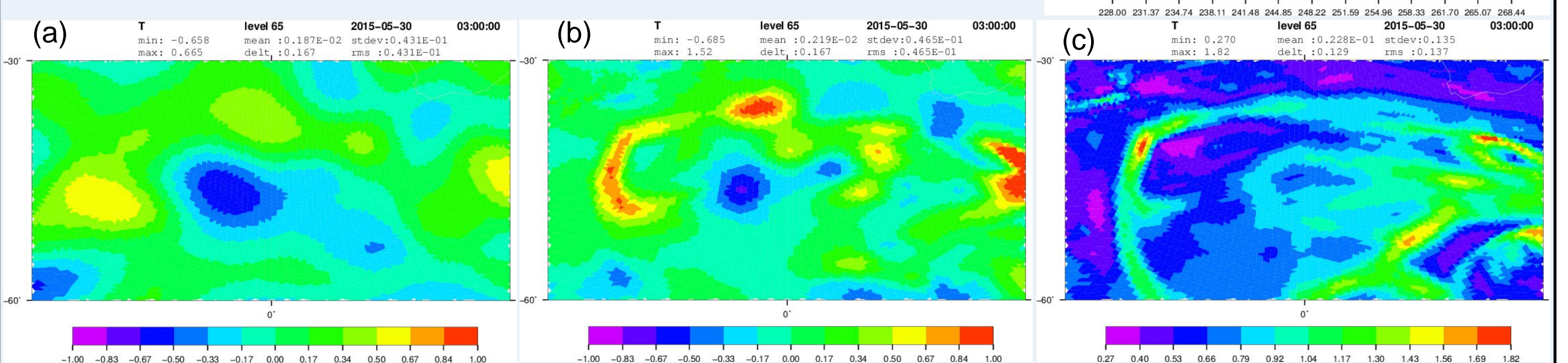


Fig 6: Example of regional T increments at around 500 hPa of 3DVar (a) in comparison to EnVar (b) together with the spread of the T fields of the ensemble (c) and the mean T field (d). While the overall pattern of analysis increments is similar, the EnVar system is able to produce much more localized increments, e.g. located within the areas of higher T uncertainty in the frontal region.



Currently, the EnVAR/LETKF system is undergoing further parameter tuning, such as the adaptation of observation errors, data thinning, and scale selective localization. Concerning the assimilation of radiances the focus is on the improvement of (situation dependent) localization and the inclusion of additional radiance data, especially humidity sensitive radiances. The EnVAR/LETKF system so far shows an improved fit to humidity observations compared to the old system. Also, the exploitation of the cross-correlations between variables, e.g. T and Qv, Qv and wind, is further investigated.

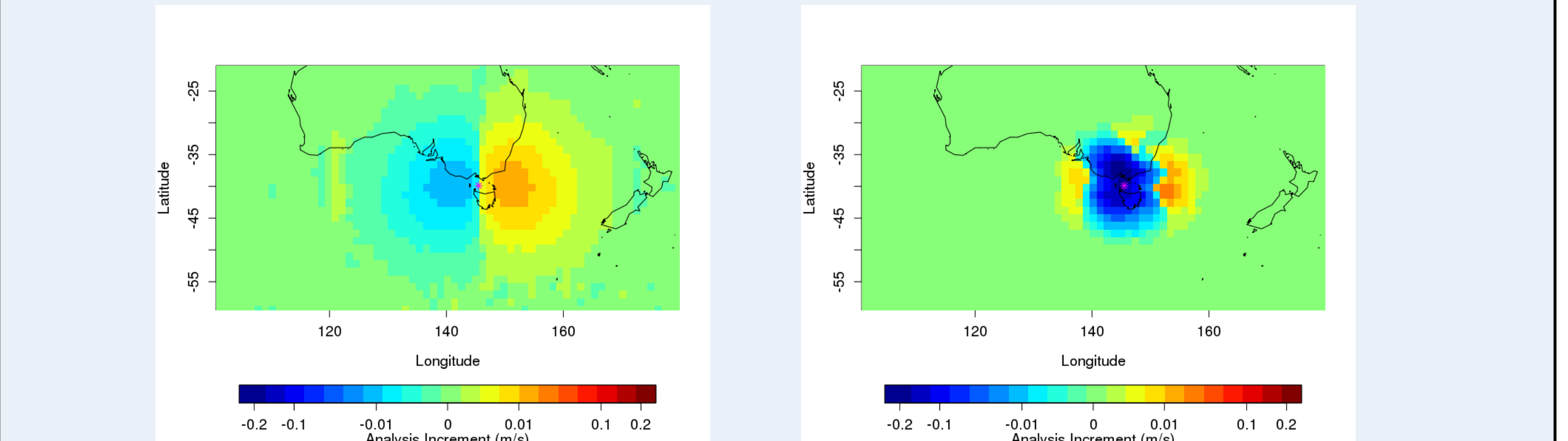


Fig 7: Example of analysis increments for wind (v-component) caused by a single radiance observation (HIRS chan 11) in 3DVar (left) and the LETKF (right). A non-linear scale is used to enhance small increment values. The 3DVar wind increment is very small in magnitude and displays the typical dipole pattern from the fixed climatological T-(u,v) correlation. In the LETKF, wind increments for these single observation tests are generally found to be much more significant and to have a highly location dependent shape and structure determined by the local T-Qv and also T-(u,v) covariances derived from the ensemble members. These covariances (and increments) vary considerably dependent on the location and meteorological conditions.

Fig 8: Example of increment profile of the v-component of the wind (in m/s) caused by a single radiance observation (HIRS channel 11) both in 3DVar (red) and in the LETKF for the ensemble mean (blue) and individual ensemble members (grey). The LETKF derives wind increments from the predominantly humidity sensitive channel in a broad coherent layer while increments in the 3DVar are negligible.

